Title page

Hydrogen sulfide protects against ischemic heart failure by inhibiting RIP1/RIP3/MLKL-mediated necroptosis

FENFEN MA[1], YAHONG ZHU[1], LINGLING CHANG[2], JINGRU GONG[1], YING LUO[1], JING DAI[3] and HUIPING LU[1]

[1]Department of Pharmacy, Shanghai Pudong Hospital, Fudan University, Shanghai 201399, China

[2]School of Pharmacy, Fudan University, Shanghai 201203, China

[3]Department of Clinical Diagnostics, Hebei Medical University, Shijiazhuang, Hebei 050017, P.R. China

Correspondence to: Dr Jing Dai, Department of Clinical Diagnostics, Hebei Medical University, 361 Zhongshan Road, Shijiazhuang, Hebei 050017, P.R. China
E-mail: 15434732@qq.com
&
Professor Huiping Lu, Department of Pharmacy, Shanghai Pudong Hospital, Fudan University, Shanghai 201399, P.R. China
E-mail: lhp310@126.com

Running title: HYDROGEN SULFIDE PROTECTS AGAINST MYOCARDIAL INFARCTION

Summary

The aim of the present study was to explore whether hydrogen sulfide (H_2S) protects against ischemic heart failure (HF) by inhibiting the necroptosis pathway. Mice were randomized into Sham, myocardial infarction (MI), MI + propargylglycine (PAG) and MI + sodium hydrosulfide (NaHS) group, respectively. The MI model was induced by ligating the left anterior descending coronary artery. PAG was intraperitoneally administered at a dose of 50 mg/kg/day for 4 weeks, and NaHS at a dose of 4mg/kg/day for the same period. At 4 weeks after MI, the following were observed: A significant decrease in the cardiac function, as evidenced by a decline in ejection fraction (EF) and fractional shortening (FS); an increase in plasma myocardial injury markers, such as creatine kinase-MB (CK-MB) and cardiac troponin I (cTNI); an increase in myocardial collagen content in the heart tissues; and a decrease of H_2S level in plasma and heart tissues. Furthermore, the expression levels of necroptosis-related markers such as receptor interacting protein kinase 1 (RIP1), RIP3 and mixed lineage kinase domain-like protein (MLKL) were upregulated after MI. NaHS treatment increased H_2S levels in plasma and heart tissues, preserving the cardiac function by increasing EF and FS, decreasing plasma CK-MB and cTNI and reducing collagen content. Additionally, NaHS treatment significantly downregulated the RIP1/RIP3/MLKL pathway. While, PAG treatment aggravated cardiac function by activated the RIP1/RIP3/MLKL pathway. Overall, the present study concluded that H_2S protected against ischemic HF by inhibiting RIP1/RIP3/MLKL-mediated necroptosis which could be a potential target treatment for ischemic HF.

Key words: hydrogen sulfide, ischemic heart failure, myocardial infarction, necroptosis, RIP1/RIP3/MLKL pathway

Introduction

It is well recognized that with altered lifestyles and growing ageing populations, heart failure (HF), the end-stage of various myocardial diseases, is associated with increasing hospitalization, high mortality and severe morbidity. Acute myocardial infarction (AMI) represents the most common cause of myocardial injury and ventricular dysfunction, accounting for a significant percentage of ischemic HF cases [1]. Percutaneous coronary intervention or thrombolytic therapy is currently the most effective strategy to improve the clinical outcome for patients with AMI; however, numerous patients still suffer from post-myocardial infarction (MI) cardiac remodeling and HF. Upon AMI, the limited oxygen supply induces ischemic cardiomyocyte necrosis, which is then replaced by scar tissue, thereby resulting in systolic dysfunction, myocardial remodeling and, finally, HF. Therefore, reducing myocardial injury and myocardial remodeling is key to delaying and treating ischemic HF [2-3].

Recently, it has been revealed that hydrogen sulfide (H_2S), a highly toxic gas, is recognized as another important endogenous gaseous signaling molecule, except in addition to nitric oxide (NO) and carbon monoxide (CO) [4]. Endogenously, H_2S is mainly generated by three key enzymes: Cystathionine β-synthase (CBS), cystathionine γ-lyase (CSE) and 3-mercaptopyruvate sulphur transferase (3-MST). Predominantly localized in the heart and vasculature, CSE is the most relevant H_2S-producing enzyme in the cardiovascular system [5-6]. At a physiological level, H_2S exerts a number of protective properties in the cardiovascular system, including anti-hypertension, anti-arteriosclerosis and anti-myocardial ischemia/reperfusion (I/R) injury [7]. It has been reported that H_2S takes part in MI [8], and that mice overexpressing CSE have a reduced infarct size compared with controls [9], while CSE knockout (KO) mice have an increased infarct size following I/R [10]. Different types of exogenous H_2S donors have been reported to improve cardiac function in mice by reducing apoptosis, inhibiting oxidative stress injury or suppressing the inflammatory response [11-12]; however, the exact mechanism is not yet fully understood.

In recent years, increasing evidence has indicated that necroptosis, a form of programmed necrosis, can be involved in the pathogenesis of cardiovascular disease, as indicated by the evidence that necroptosis contributes to the development of atherosclerosis, myocardial I/R injury and stroke [13-15]. Necroptosis has been

reported to mediate adverse remodeling after MI, and has been identified in the etiology of various types of human HF [16-17]. In addition, cardiac function is improved by necrostatin-1, a small molecule inhibitor of necroptosis after I/R injury [18]. However, to the best of our knowledge, whether necroptosis inhibition is involved in the myocardial protection effect of H_2S has not yet been fully investigated. Therefore, in the present study, propargylglycine (PAG), a CSE inhibitor, was used to inhibit the production of endogenous H_2S and sodium hydrosulfide (NaHS) was used as an exogenous donor of H_2S to explore whether H_2S is capable of protecting against ischemic HF by inhibiting the necroptosis pathway.

Materials and Methods

Animals and experimental protocol.

Adult male C57BL/6 mice (weight, 20-22 g; age, 8 weeks) were acquired from Gempharmatech Co., Ltd. Mice were housed under pathogen-free conditions with a controlled humidity of 60%, at 22-24˚C and under a regular 12-h light/dark cycle, with *ad libitum* access to food and water. All animal procedures (approval no. WZ-011) were approved by the Ethics Committee of Experimental Research, Shanghai Pudong Hospital of Fudan University (Shanghai, China) and were performed according to the Guide for the Care and Use of Laboratory Animals published by the National Institutes of Health.

After 1 week of acclimating, the 64 mice were randomly assigned into 4 groups: Sham, MI, MI + PAG, and MI + NaHS groups. PAG was intraperitoneally administered at a dose of 50 mg/kg/day for 4 weeks; NaHS, at a dose of 4 mg/kg/day for the same period. The Sham and MI group were intraperitoneally administered the equivalent volume of saline at the same time points.

Myocardial ischemia mouse model.

The MI model was induced by ligating the left anterior descending coronary artery (LAD) as previously described [19]. Isoflurane was used at 2% concentration for the induction of anesthesia and at 1.5% concentration for the maintenance of anesthesia. And then the mice were ventilated via tracheal intubation with a rodent ventilator (Kent Scientific Corporation). With the chest opened, MI was achieved by occluding LAD the using a 7-0 silk suture. Successful ligation of the LAD was confirmed by ST-segment shift on the ECG and the anterior wall of the left ventricle turned pale. Mice in the Sham group underwent the same surgery without LAD ligation, and the chest was closed in layers after surgery.

Echocardiographic study.

Under isoflurane anesthesia, transthoracic echocardiography was performed using a Vevo2100 ultrasound device (VisualSonics, Inc.) at 4 weeks after MI, with two-dimensional guided M-mode images being recorded and left ventricular ejection fraction (LVEF) and left ventricular fractional shortening (LVFS) measured to

evaluate heart function, which were calculated from the following formulas: (1) EF (%) = 100 × {[LV end-diastolic volume (LVEDV) - LV end-systolic volume (LVESV)]/LVEDV}; (2) FS (%) = 100 ×{[LV end-diastolic dimension (LVEDD) - LV end-systolic dimension (LVESD)]/LVEDD}. All measurements were averaged for three consecutive cardiac cycles. After echocardiographic measurements described as aforementioned, the mice were euthanized by an overdose of pentobarbital (100 mg/kg; intraperitoneal injection). Subsequently, the heart was rapidly removed and retained at -80˚C until further analysis. After centrifugation at 1,200 x g and 4˚C for 10 min, plasma was separated from the blood and frozen at -80˚C until the following assays.

Measurement of plasma creatine kinase-MB (CK-MB) and cardiac troponin I (cTnI).

The plasma levels of CK-MB were determined with an automatic biochemical analyzer (Cobas 6000; Roche Diagnostics). The levels of cTnI in the plasma were measured using ELISA kits (cat. no. MM-0791M1; Jiangsu Meimian Industrial Co., Ltd.) according to the manufacturer's instructions.

Measurement of H_2S.

H_2S levels in the heart tissues and plasma were measured using liquid chromatography-mass spectrometry (LC-MS/MS) as previously described [20]. The heart tissues were homogenized in the ice cold Tris-HCl (100 mmol/l; pH 8.5), followed by centrifugation at 12,000 x g for 20 min at 4˚C; the protein in the supernatant was quantified using BCA reagent (Sigma-Aldrich; Merck KGaA), with 30 µL supernatant or plasma, 80 µl monobromobimane (Sigma-Aldrich; Merck KGaA) and 10 µL ammonia (0.1%) shaken to be mixed at room temperature for 1 h, and an addition of 10 µL formic acid (20%) to stop the reaction. Following a 10 min centrifugation (12,500 x g; 4˚C), the supernatants were stored at -80˚C until H_2S measurements were performed. Sodium sulfide (0-40 µmol/l) was used to make the standard curve to determine H_2S concentration. In the heart tissues, H_2S concentration was divided by the protein concentration and expressed as 0.01 nM/mg of protein.

Hematoxylin and eosin (H&E) staining and Sirius red staining.

The mouse hearts were isolated and fixed in 4% paraformaldehyde (pH 7.4) at room temperature for 24 h. H&E staining and Sirius Red staining were performed after dehydration, permeabilization with xylene, wax dipping, paraffin embedding and 5-μm sectioning of the heart tissues. H&E staining was performed at room temperature after dewaxing for 80 min. Briefly, nuclei were stained with hematoxylin for 5 min, cytoplasm was stained with eosin for 3 min, and samples were dehydrated and sealed for 25 min. Sirius red staining was performed at room temperature after dewaxing for 80 min. Briefly, samples were stained with Sirius red for 10 min, followed by dehydration and sealing for 5 min. H&E staining was performed to observe histopathological changes, and Sirius red staining was performed to evaluate collagen deposition. The protocols for HE staining and Sirius red staining were conducted according to the manufacturer's instructions (cat. nos. G1120 and G1470; Beijing Solarbio Science & Technology Co., Ltd.), and images were captured under an optical microscope (Zeiss, Inc.).

Immunohistochemistry.

The mouse hearts were isolated and fixed in 4% paraformaldehyde (pH 7.4) at room temperature for 24 h and were embedded in paraffin. When dewaxed, the paraffin-embedded sections of the heart tissues (5-μm) were rehydration in a descending alcohol series was then performed retrieved using a pressure cooker at 125 ˚C for 12 min in citrate buffer (pH 6.0), 0.01M PBS (pH 7.4) was used as a washing reagent .And the sections were blocked in 3% BSA (cat. no. B2064; Sigma-Aldrich; Merck KGaA) at room temperature for 30 min. Subsequently, the sections were incubated with receptor interacting protein kinase 1 (RIP1; cat. no. ab106393; 1:200; Abcam) or receptor interacting protein kinase 3 (RIP3; cat. no. ab62344; 1:200; Abcam) antibodies (1:200; Abcam) at room temperature for 2 h, before being incubated with horseradish peroxidase (HRP)-conjugated secondary antibody (cat. no. K5007; Dako; Agilent Technologies, Inc.) at room temperature for 30 min and diaminobenzidine substrate. Consequently, at least five random fields of each section were examined under a light microscope (Leica Microsystems GmbH).

Western blotting.

Protein was extracted from the left ventricle tissues using RIPA buffer (1% Triton X-100, 150 mM NaCl, 5 mM EDTA and 10 mM Tris-HCl, pH 7.0; Beyotime Institute of Biotechnology) and quantified using BCA reagent (cat. no. 71285-3; MilliporeSigma) The protein samples (80 µg/lane) were subjected to 10% SDS-PAGE gels and then transferred to polyvinylidene fluoride membranes. After blocking with 5% non-fat milk at room temperature for 1 h, the membranes were incubated with primary antibodies against RIP1 (cat. no. ab106393; 1:200; Abcam), RIP3 (cat. no. ab62344; 1:200; Abcam), mixed lineage kinase domain-like protein (MLKL; cat. no. ab243142; 1:1,000; Abcam) and GAPDH as the internal control (cat. no. 5174S; 1:2,000; Cell Signaling Technology, Inc.) at 4˚C overnight. After washing with TBS-0.2% Tween thrice, the membranes were incubated with HRP-conjugated secondary antibodies [Anti-rabbit IgG, HRP-linked Antibody (cat. no. 7074; 1:3,000; Cell Signaling Technology, Inc.); Goat Anti-Rat IgG, Light-Chain Specific Antibody (HRP Conjugate) (cat. no. 98164; 1:3,000; Cell Signaling Technology, Inc.)] at room temperature for 1 h. Chemiluminescent signals were developed by the addition of the enhanced chemiluminescence reagents (Bio-Rad Laboratories, Inc.). The intensities of protein bands were quantified using ImageJ software (version 1.8.0_172; National Institutes of Health).

Statistical analyses.

The results are presented as mean ± SEM (n=6). Statistical analysis was performed using an SPSS software package, version 25.0 (SPSS, Inc.). The results of ≥3 groups were compared using one-way ANOVA followed by Tukey's post hoc test. $P<0.05$ was considered to indicate a statistically significant difference.

Results

H_2S levels decrease after MI. As presented in Fig. 1, a significant decrease was observed in H_2S levels of the plasma (Fig. 1A) and heart tissues (Fig. 1B) after MI compared with the Sham group. This was decreased significantly further by treatment with PAG (a CSE inhibitor) and significantly partially reversed by NaHS (an exogenous donor of H_2S) treatment. Furthermore, the myocardial injury markers of plasma CK-MB (Fig. 1C) and cardiac troponin I (cTNI; Fig. 1D) increased significantly after MI compared with the Sham group; notably, PAG treatment significantly enhanced the level of CK-MB and cTNI further, while NaHS treatment partially reversed such results.

Cardiac function is preserved by H_2S after MI. According to the echocardiography on the cardiac function (Fig. 2), MI significantly decreased ejection fraction (EF) and fractional shortening (FS) compared with the Sham group; consequently, NaHS treatment preserved the cardiac function, while PAG treatment aggravated the decline of EF and FS after MI.

Myocardial remodeling is inhibited by H_2S after MI. As presented in Fig. 3 and S1, Sirius red staining was performed to identify the areas of collagen deposition and fibrosis content, and H&E staining was performed to observe histopathological changes in the heart tissue. An increase in collagen accumulation and fibrosis content was observed in the MI group compared with the Sham group. After MI, the mice treated with NaHS demonstrated a reduction in collagen accumulation and fibrosis content, while those treated with PAG presented an increase. In addition, as presented in Table SI, the diastolic and systolic left ventricular anterior wall (LVAW) of MI mice was significantly reduced compared with the sham mice. PAG treatment significantly aggravated the decline of diastolic and systolic LVAW compared with the MI group, while NaHS treatment significantly ameliorated this reduction compared with the MI group.

RIP1/RIP3/MLKL-mediated necroptosis is reduced by H_2S after MI. To examine whether necroptosis was involved in MI, immunohistochemical staining was performed to evaluate the expression levels of RIP1 and RIP3, the results of which demonstrated that RIP1 and RIP3-positive cells were stained brown (Fig. 4A-D). The

expression levels of RIP1 and RIP3 were revealed to be low in the Sham group, whereas a significantly increased number of RIP1 and RIP3-positive cells were observed in the MI group, which was increased further by PAG treatment. However, NaHS treatment significantly decreased the number of RIP1 and RIP3-positive cells compared with the MI group. As indicated by western blotting, the expression levels of RIP1, RIP3 and MLKL were upregulated in the MI group compared with the Sham group (Fig. 4E-G). The administration of NaHS resulted in a significant decrease of these expression levels compared with the MI group, while PAG treatment led to a significant increase.

Discussion

The present study revealed that H_2S significantly improved myocardial ischemic injury, enhanced myocardial function and inhibited cardiac remodeling in mice with ischemic HF that had undergone LAD ligation. Furthermore, the present study provided evidence that H_2S down-regulated the expression of the RIP1/RIP3/MLKL pathway, thus inhibiting necroptosis activation in ischemic HF. These findings suggested that H_2S could be a potential target treatment for ischemic HF by inhibiting RIP1/RIP3/MLKL-mediated necroptosis.

Being the most severe form of coronary artery disease, MI accounts for a major cause of cardiovascular morbidity and mortality in the increasingly ageing populations worldwide. When MI occurs, the severe reduction in coronary perfusion causes a loss of a large number of myocardial cells, which further leads to cardiac remodeling in the form of scar formation, myocardial fibrosis and poor ventricular dilatation and irreversible HF in the late phase [21-22]. Animal models have been developed to study molecular mechanism or therapeutic strategies for HF after MI. Since surgical occlusion of the LAD coronary artery is a well-established model for initiating an MI in rodent models, the present study used the model of HF post-MI developed by a 4-week permanent ligation of the LAD as previously described [20]. At 4 weeks after MI, the cardiac function was evaluated using echocardiography, the results of which demonstrated that MI significantly decreased EF and FS compared with the Sham group; while the plasma levels of the myocardial injury markers of CK-MB and cTNI were significantly increased after MI. Additionally, the results of H&E staining and Sirius red staining revealed an increase in the collagen accumulation and fibrosis content of the MI group. These results clearly indicated that HF could be successfully induced at 4 weeks after MI, which were in parallel with the results of the previously reported studies [23-24].

At present, interventional and pharmacological therapies of MI aim to restore blood supply as soon as possible in the infarcted heart so as to significantly decrease the initial cardiac damage. However, MI patients are still at a high risk of subsequent death due to HF [25]. Thus, there is an unmet need for novel therapeutic candidates that can prevent and delay the occurrence and development of ischemic HF. Our previous study demonstrated that S-propargyl-cysteine can exert a protective effect on AMI by prolonging the release of endogenous H_2S via the CSE/H_2S pathway [26]. The present study investigated the cardioprotective effect of H_2S on ischemic HF after

4 weeks of administration of NaHS (4 mg/kg/day), an exogenous donor of H_2S, or PAG (50 mg/kg/day), a CSE inhibitor. H_2S, which is a colorless toxic gas, is now considered to be the third most important endogenous gasotransmitter that can freely cross the cell membrane following NO and CO, and be endogenously synthesized in mammalian tissues by the three enzymes of CSE, CBS and 3-MST. A decrease in the endogenous production of H_2S, which plays a physiological role in a variety of cellular and organic functions, has been associated with some pathological conditions involving various systems, including the cardiovascular system. In the heart, H_2S is mainly produced via CSE and has been reported to provide a cardioprotective effect in various cardiac injury models, while CSE KO mice or the application of CSE inhibitor PAG can aggravate the corresponding cardiac injury [27-28]. The present study demonstrated a significant decrease in H_2S levels post-MI in the MI group of plasma and heart tissues compared with the Sham group, which was successfully reversed by NaHS treatment. NaHS treatment also preserved the cardiac function by increasing EF and FS, decreasing plasma myocardial injury markers, such as CK-MB and cTNI, and reducing collagen accumulation and fibrosis content.

By contrast, PAG treatment inhibited the endogenous production of H_2S, causing a further reduction in H_2S levels of plasma and heart tissues. Moreover, PAG treatment aggravated the cardiac function by decreasing EF and FS, increasing plasma CK-MB and cTNI levels and enhancing collagen accumulation and fibrosis content. These results were supported by our previous research, which revealed that H_2S supplementation can ameliorate pathological remodeling and the cardiac dysfunction of the wild-type and CSE KO mice in post-MI HF or isoprenaline-induced HF [29-30]. These results were also consistent with previously reported investigations that indicated that H_2S deceases MI injury and inhibits cardiac remodeling through a complex mechanism involving antioxidant, anti-apoptotic, anti-inflammatory and anti-fibrotic effects [31-32]. However, the exact mechanism has not yet been fully understood.

Cell death is a fundamental process in cardiac pathologies and multiple forms of cell death mechanisms have been identified, including apoptosis, necroptosis, ferroptosis and pyroptosis [33]. Necroptosis, a recently identified type of programmed cell death, is a lytic form of cell death distinguished from apoptosis, ferroptosis and pyroptosis. Different from other forms of cell death, necroptosis is orchestrated by complex IIb (also called necrosome), which includes RIP1, RIP3 and MLKL;

RIP1/RIP3/MLKL signaling is considered the canonical signaling module for necroptosis [33-35]. The critical event in the induction of necroptosis is the activation of RIP3, a serine/threonine kinase, which is often activated through phosphorylation carried out by the homologous RIP1. Afterwards, RIP3 phosphorylates and activates MLKL, which translocates to and permeabilizes the plasma membrane to induce necroptosis [34]. So, a general way to assess necroptosis signaling is to measure the protein levels of RIP3, MLKL, and RIP1, and their phosphorylation state are also measured to identity necroptosis [36].

Some studies have suggested that necroptosis plays an instrumental role, contributing to cardiovascular diseases and fatalities, and that the genetic deletion or pharmacological inhibition of RIP1/RIP3/MLKL pathway has a protective effect [16, 37]. By contrast, it has been reported that cardiac-specific overexpression of RIP3 aggravated necrotic cardiomyocyte death, post-MI cardiac remodeling and cardiac dysfunction [38]. The present study demonstrated that the RIP1/RIP3/MLKL pathway was upregulated in the MI group compared with the Sham group and this corresponded with previous study which reported the RIP1, RIP3, and MLKL expression were up-regulated after myocardial I/R injury, while necrostatin-1, a RIP1 inhibitor, could inhibit RIP1-dependent necrosis after myocardial I/R in vivo and prevent adverse cardiac remodeling [39]. In addition, the phosphorylated RIP1, RIP3, and MLKL were measured and they were all up-regulated after MI (Supplementary Fig. S2). The present study also revealed that NaHS treatment significantly downregulated the RIP1/RIP3/MLKL pathway, while PAG treatment further activated RIP1/RIP3/MLKL pathway. These results indicated that H_2S could inhibit RIP1/RIP3/MLKL-mediated necroptosis, which was consistent with our previous study where H_2S was evidenced to mitigate endoplasmic reticulum stress-related necroptosis by downregulating the RIP3-CaMKII signaling pathway in a AMI injury model [40]. Additionally, a previously reported *in vitro* experiment demonstrated that H_2S protects HUVECs against high glucose-induced injury by inhibiting necroptosis [41], while Chi *et al* [42] revealed that H_2S exposure induces necroptosis, promoting inflammation through the MAPK/NF-κB pathway in broiler spleen. Therefore, further in-depth research is needed to be conducted on H_2S. In conclusion, the present study verified that H_2S could protect against ischemic HF by inhibiting RIP1/RIP3/MLKL-mediated necroptosis, suggesting that such a finding may offer a potential treatment target for ischemic HF.

Acknowledgements

No applicable.

Funding

The present study was supported by the Natural Science Foundation of China (grant no. 81900224); Shanghai Rising Stars of Medical Talent Youth Development Program/Youth Medical Talents/Clinical Pharmacist Program (grant no. SHWRS [2020]_087); the fund of Research Grant for Health Science and Technology of Shanghai Municipal Commission of Health Committee (grant no. 20214Y0268); the fund of Academic Leaders Training Program of Pudong Health Committee of Shanghai (grant no. PWRd2017-11); the Major Weak Discipline Construction Project of Pudong Health and Family Planning Commission of Shanghai (grant no. PWZbr2017-15); Science and Technology Development Fund of Shanghai Pudong New Area (grant no. PKJ2018-Y37); Talents Training Program of Pudong Hospital Affiliated to Fudan University (grant no. PX201704); Science and Technology Development Fund of Shanghai Pudong New Area (grant no. PKJ2020-Y49); Fudan Zhangjiang Clinical Medicine Innovation Fund Project (grant no. KP7202112 & KP0202121); and Shanghai Medical Institution Clinical Pharmacy Key Specialized Subject Construction Project (District).

Availability of data and materials

The datasets used and/or analyzed during the current study were available from the corresponding author on reasonable request.

Authors' contributions

FM designed and performed the experiments, analyzed the data and wrote the manuscript. JG and YZ designed and performed the western blotting, and H&E and Sirius red staining. YL performed some of the animal model-based experiments and western blotting. HL and JD designed the study and supervised the project. FM and HL confirm the authenticity of all the raw data. FM and YZ contributed to this work equally. All authors have read and approved the final manuscript.

Ethics approval and consent to participate

All animal procedures were approved by the Ethics Committee of Experimental

Research, Shanghai Pudong Hospital of Fudan University, and were performed according to the Guide for the Care and Use of Laboratory Animals published by the National Institutes of Health (approval no. WZ-011; Shanghai, China).

Patient consent for publication

Not applicable.

Competing interests

The authors declare that they have no competing interests.

References

1. Dunlay SM, Roger VL. Gender differences in the pathophysiology, clinical presentation, and outcomes of ischemic heart failure. Curr Heart Fail Rep. 2012;9(4):267-276.
2. Domengé O, Ragot H, Deloux R, et al. Efficacy of epicardial implantation of acellular chitosan hydrogels in ischemic and nonischemic heart failure: impact of the acetylation degree of chitosan. Acta Biomater. 2021;119:125-139.
3. Yan W, Lin C, Guo Y, et al. N-Cadherin Overexpression Mobilizes the Protective Effects of Mesenchymal Stromal Cells Against Ischemic Heart Injury Through a β-Catenin-Dependent Manner. Circ Res. 2020;126(7):857-874.
4. Ali A, Wang Y, Wu L, Yang G. Gasotransmitter signaling in energy homeostasis and metabolic disorders. Free Radic Res. 2021;55(1):83-105.
5. Pan LL, Liu XH, Gong QH, Yang HB, Zhu YZ. Role of cystathionine γ-lyase/hydrogen sulfide pathway in cardiovascular disease: a novel therapeutic strategy?. Antioxid Redox Signal. 2012;17(1):106-118.
6. Hsu CN, Tain YL. Preventing Developmental Origins of Cardiovascular Disease: Hydrogen Sulfide as a Potential Target?. Antioxidants (Basel). 2021;10(2):247.
7. Zhang H, Dai J, Tian D, et al. Hydrogen Sulfide Restored the Diurnal Variation in Cardiac Function of Aging Mice. Oxid Med Cell Longev. 2021;2021:8841575.
8. Donnarumma E, Trivedi RK, Lefer DJ. Protective Actions of H2S in Acute Myocardial Infarction and Heart Failure. Compr Physiol. 2017. 7(2): 583-602.
9. Calvert JW, Elston M, Nicholson CK, et al. Genetic and pharmacologic hydrogen sulfide therapy attenuates ischemia-induced heart failure in mice. Circulation. 2010;122(1):11-19.
10. Miao L, Xin X, Xin H, Shen X, Zhu YZ. Hydrogen Sulfide Recruits Macrophage Migration by Integrin β1-Src-FAK/Pyk2-Rac Pathway in Myocardial Infarction [published correction appears in Sci Rep. 2022 Feb 2;12(1):2109]. Sci Rep. 2016;6:22363.
11. Donnarumma E, Bhushan S, Bradley JM, et al. Nitrite Therapy Ameliorates Myocardial Dysfunction via H_2S and Nuclear Factor-Erythroid 2-Related Factor

2 (Nrf2)-Dependent Signaling in Chronic Heart Failure. J Am Heart Assoc. 2016;5(8):e003551.

12. Kar S, Kambis TN, Mishra PK. Hydrogen sulfide-mediated regulation of cell death signaling ameliorates adverse cardiac remodeling and diabetic cardiomyopathy. Am J Physiol Heart Circ Physiol. 2019;316(6):H1237-H1252.
13. Rasheed A, Robichaud S, Nguyen MA, et al. Loss of MLKL (Mixed Lineage Kinase Domain-Like Protein) Decreases Necrotic Core but Increases Macrophage Lipid Accumulation in Atherosclerosis. Arterioscler Thromb Vasc Biol. 2020;40(5):1155-1167.
14. Ying L, Benjanuwattra J, Chattipakorn SC, Chattipakorn N. The role of RIPK3-regulated cell death pathways and necroptosis in the pathogenesis of cardiac ischaemia-reperfusion injury. Acta Physiol (Oxf). 2021;231(2):e13541.
15. Zhang Y, Li M, Li X, et al. Catalytically inactive RIP1 and RIP3 deficiency protect against acute ischemic stroke by inhibiting necroptosis and neuroinflammation. Cell Death Dis. 2020;11(7):565.
16. Luedde M, Lutz M, Carter N, et al. RIP3, a kinase promoting necroptotic cell death, mediates adverse remodelling after myocardial infarction. Cardiovasc Res. 2014;103(2):206-216.
17. Szobi A, Gonçalvesová E, Varga ZV, et al. Analysis of necroptotic proteins in failing human hearts [published correction appears in J Transl Med. 2017 May 11;15(1):103]. J Transl Med. 2017;15(1):86.
18. Koudstaal S, Oerlemans MI, Van der Spoel TI, et al. Necrostatin-1 alleviates reperfusion injury following acute myocardial infarction in pigs. Eur J Clin Invest. 2015;45(2):150-159.
19. Kuhn TC, Knobel J, Burkert-Rettenmaier S, et al. Secretome Analysis of Cardiomyocytes Identifies PCSK6 (Proprotein Convertase Subtilisin/Kexin Type 6) as a Novel Player in Cardiac Remodeling After Myocardial Infarction. Circulation. 2020;141(20):1628-1644.
20. Tan B, Jin S, Sun J, et al. New method for quantification of gasotransmitter hydrogen sulfide in biological matrices by LC-MS/MS. Sci Rep. 2017;7:46278.

21. Gabriel-Costa D. The pathophysiology of myocardial infarction-induced heart failure. Pathophysiology. 2018;25(4):277-284.
22. Mouton AJ, Rivera OJ, Lindsey ML. Myocardial infarction remodeling that progresses to heart failure: a signaling misunderstanding. Am J Physiol Heart Circ Physiol. 2018;315(1):H71-H79.
23. Matsushima S, Ide T, Yamato M, et al. Overexpression of mitochondrial peroxiredoxin-3 prevents left ventricular remodeling and failure after myocardial infarction in mice. Circulation. 2006;113(14):1779-1786.
24. Pan Y, Zhou Z, Zhang H, et al. The ATRQβ-001 vaccine improves cardiac function and prevents postinfarction cardiac remodeling in mice. Hypertens Res. 2019;42(3):329-340.
25. Bucholz EM, Butala NM, Rathore SS, Dreyer RP, Lansky AJ, Krumholz HM. Sex differences in long-term mortality after myocardial infarction: a systematic review. Circulation. 2014;130(9):757-767.
26. Tran BH, Huang C, Zhang Q, et al. Cardioprotective effects and pharmacokinetic properties of a controlled release formulation of a novel hydrogen sulfide donor in rats with acute myocardial infarction. Biosci Rep. 2015;35(3):e00216.
27. Zhang Z, Jin S, Teng X, Duan X, Chen Y, Wu Y. Hydrogen sulfide attenuates cardiac injury in takotsubo cardiomyopathy by alleviating oxidative stress. Nitric Oxide. 2017;67:10-25.
28. Shimizu Y, Polavarapu R, Eskla KL, et al. Hydrogen sulfide regulates cardiac mitochondrial biogenesis via the activation of AMPK. J Mol Cell Cardiol. 2018;116:29-40.
29. Miao L, Shen X, Whiteman M, et al. Hydrogen Sulfide Mitigates Myocardial Infarction via Promotion of Mitochondrial Biogenesis-Dependent M2 Polarization of Macrophages. Antioxid Redox Signal. 2016;25(5):268-281.
30. Wu D, Hu Q, Xiong Y, Zhu D, Mao Y, Zhu YZ. Novel H2S-NO hybrid molecule (ZYZ-803) promoted synergistic effects against heart failure. Redox Biol. 2018;15:243-252.
31. Kar S, Shahshahan HR, Kambis TN, et al. Hydrogen Sulfide Ameliorates

Homocysteine-Induced Cardiac Remodeling and Dysfunction. Front Physiol. 2019;10:598.

32. Karwi QG, Whiteman M, Wood ME, Torregrossa R, Baxter GF. Pharmacological postconditioning against myocardial infarction with a slow-releasing hydrogen sulfide donor, GYY4137. Pharmacol Res. 2016;111:442-451.
33. Mishra PK, Adameova A, Hill JA, et al. Guidelines for evaluating myocardial cell death. Am J Physiol Heart Circ Physiol. 2019. 317(5): H891-H922.
34. Khoury MK, Gupta K, Franco SR, Liu B. Necroptosis in the Pathophysiology of Disease. Am J Pathol. 2020;190(2):272-285.
35. Sun W, Wu X, Gao H, et al. Cytosolic calcium mediates RIP1/RIP3 complex-dependent necroptosis through JNK activation and mitochondrial ROS production in human colon cancer cells. Free Radic Biol Med. 2017;108:433-444.
36. Lichý M, Szobi A, Hrdlička J, Horváth C, Kormanová V, Rajtík T, Neckář J, Kolář F, Adameová A. Different signalling in infarcted and non-infarcted areas of rat failing hearts: A role of necroptosis and inflammation. J Cell Mol Med. 2019 Sep;23(9):6429-6441.
37. Guo X, Yin H, Li L, et al. Cardioprotective Role of Tumor Necrosis Factor Receptor-Associated Factor 2 by Suppressing Apoptosis and Necroptosis. Circulation. 2017;136(8):729-742.
38. Zhang H, Yin Y, Liu Y, et al. Necroptosis mediated by impaired autophagy flux contributes to adverse ventricular remodeling after myocardial infarction. Biochem Pharmacol. 2020 May;175:113915.
39. Oerlemans MI, Liu J, Arslan F, et al. Inhibition of RIP1-dependent necrosis prevents adverse cardiac remodeling after myocardial ischemia-reperfusion in vivo. Basic Res Cardiol. 2012 Jul;107(4):270.
40. Chang L, Wang Z, Ma F, et al. ZYZ-803 Mitigates Endoplasmic Reticulum Stress-Related Necroptosis after Acute Myocardial Infarction through Downregulating the RIP3-CaMKII Signaling Pathway. Oxid Med Cell Longev. 2019;2019:6173685.
41. Lin J, Chen M, Liu D, et al. Exogenous hydrogen sulfide protects human

umbilical vein endothelial cells against high glucose-induced injury by inhibiting the necroptosis pathway. Int J Mol Med. 2018;41(3):1477-1486.

42. Chi Q, Wang D, Hu X, Li S, Li S. Hydrogen Sulfide Gas Exposure Induces Necroptosis and Promotes Inflammation through the MAPK/NF-κB Pathway in Broiler Spleen. Oxid Med Cell Longev. 2019;2019:8061823.

Figures and Figure legends

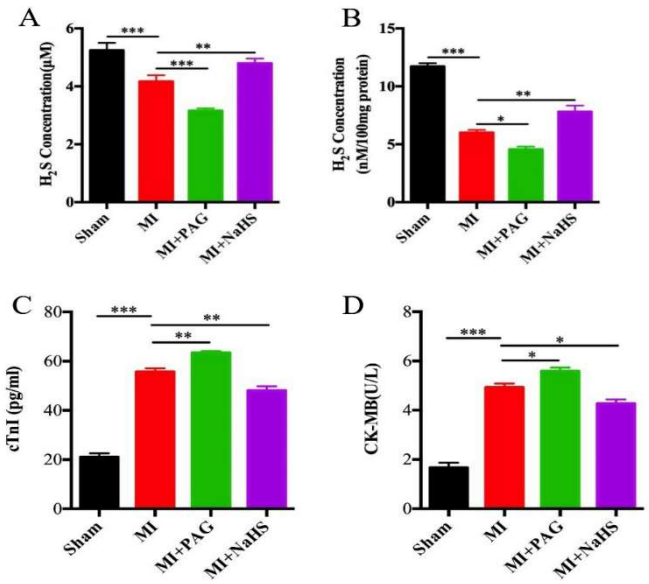

Fig. 1. H_2S levels decrease after MI and H_2S has a protective effect on MI mice in vivo. H_2S levels in (A) blood plasma and (B) heart tissues. (C) cTnI and (D) CK-MB levels in the blood plasma. Mean ± SEM. *P<0.05, **P<0.01, ***P<0.001. cTnI, cardiac troponin I; CK-MB, Creatine kinase-MB; MI, myocardial infarction; PAG, propargylglycine; NAHS, sodium hydrosulfide; H_2S, hydrogen sulfide.

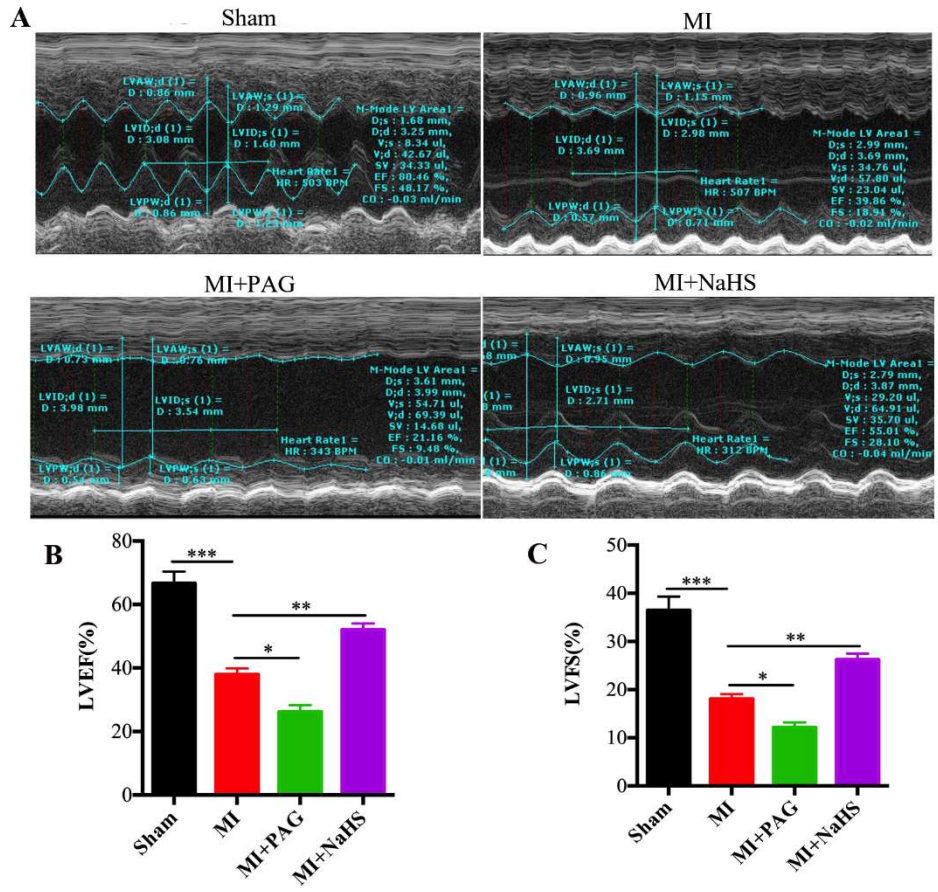

Fig. 2. H_2S treatment preserves cardiac function after MI. (A) Representative M-mode images. (B) Changes of the LVEF and (C) LVFS. Mean ± SEM. *P<0.05, **P<0.01, ***P<0.001. LVEF, left ventricular ejection fraction; LVFS, left ventricular fractional shortening; MI, myocardial infarction; PAG, propargylglycine; NAHS, sodium hydrosulfide; H_2S, hydrogen sulfide.

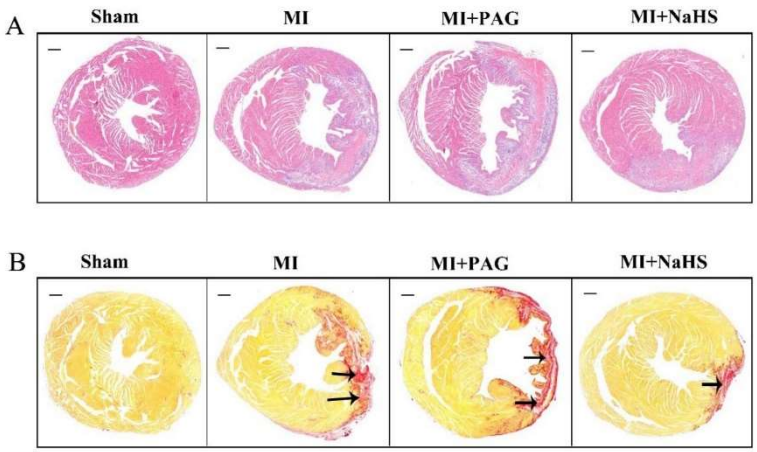

Fig. 3. H_2S treatment inhibits myocardial remodeling after MI. (A) Representative hematoxylin and eosin-stained sections. (B) Representative Sirius-red-stained sections. Red-stained collagen fibers are indicated with black arrows. Scale bar, 2.5 mm. MI, myocardial infarction; PAG, propargylglycine; NAHS, sodium hydrosulfide.

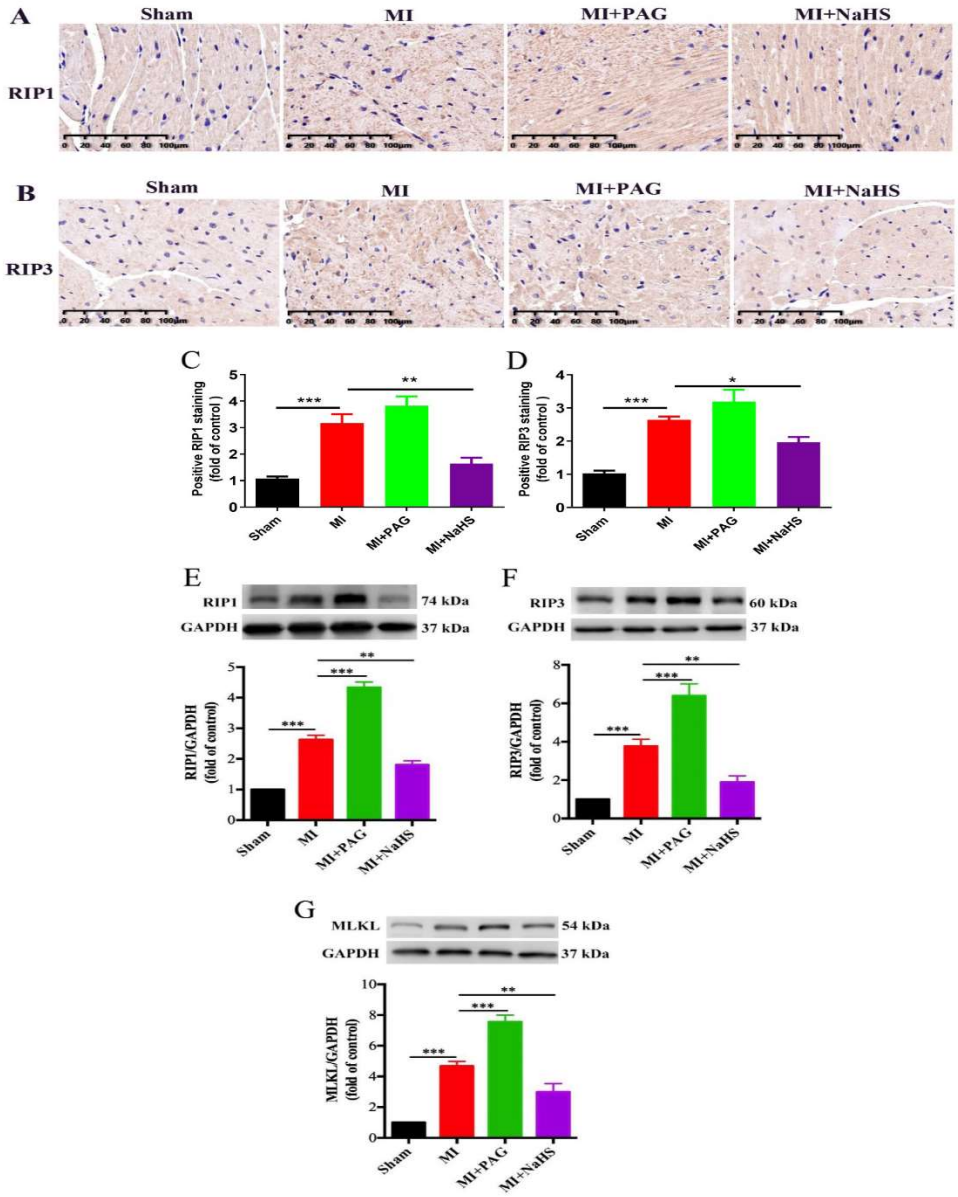

Fig. 4. H_2S treatment reduces RIP1/RIP3/MLKL-mediated necroptosis after MI. Representative immunohistochemistry for (A) RIP1 and (B) RIP3-positive cells in ischemic heart tissues. Scale bar, 100 μm. Quantitative analysis for (C) RIP1 and (D) RIP3-positive cells in ischemic heart tissues after staining. Representative western blots and quantitative analysis for (E) RIP1, (F) RIP3 and (G) MLKL expression levels in ischemic heart tissues. GAPDH was used as the internal control. Mean ± SEM. *P<0.05, **P<0.01, ***P<0.001. RIP, receptor interacting protein kinase; MLKL, mixed lineage kinase domain-like protein; MI, myocardial infarction; PAG, propargylglycine; NAHS, sodium hydrosulfide; H_2S, hydrogen sulfide.

Supplementary

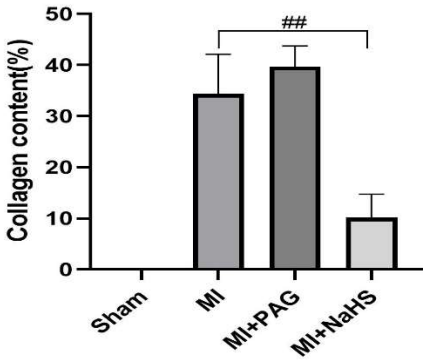

Fig. S1. H_2S inhibits myocardial remodeling after MI. (A) Sirius red was used to assess collagen content. Quantitative analysis for Sirius-red-stained sections. Mean ± SEM. $^{\#\#}P<0.01$. MI, myocardial infarction; PAG, propargylglycine; NAHS, sodium hydrosulfide; H_2S, hydrogen sulfide

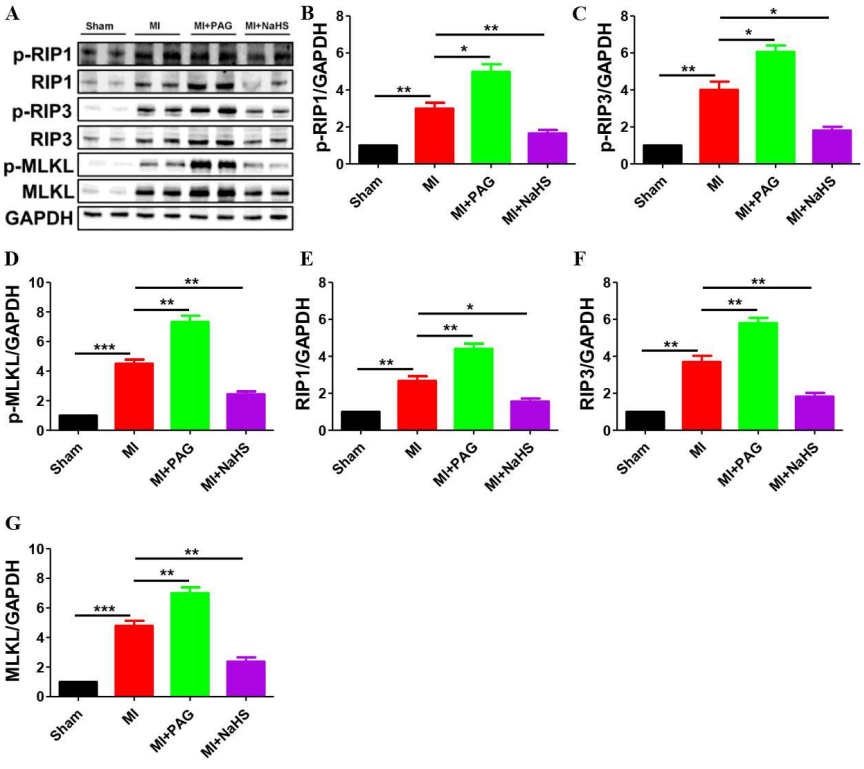

Fig. S2. H_2S treatment mitigates RIP1/RIP3/MLKL-mediated necroptosis after MI. Representative western blots (A) and quantitative analysis for (B)p-RIP1, (C)p-RIP3, (D)p-MLKL, (E) RIP1, (F) RIP3 and (G) MLKL expression levels in ischemic heart tissues. GAPDH was used as the internal control. Mean ± SEM. *P<0.05, **P<0.01, ***P<0.001. RIP, receptor interacting protein kinase; MLKL, mixed lineage kinase domain-like protein; MI, myocardial infarction; PAG,

propargylglycine; NAHS, sodium hydrosulfide; H_2S, hydrogen sulfide.

Table S1. Echocardiographic structural data.

Measurement	Sham	MI	MI + PAG	MI + NaHS
LVAW;d(I)(mm)	1.08±0.1	0.69±0.03[a]	0.62±0.03[b]	0.98±0.04[b]
LVPW;d(I)(mm)	0.94±0.05	0.49±0.03	0.55±0.02	1.01±0.05
LVAW;s(I)(mm)	1.29±0.08	0.86±0.15[a]	0.64±0.04[b]	1.01±0.05[b]
LVPW;s(I)(mm)	1.26±0.01	0.70±0.01	0.64±0.05	0.93±0.02

Data are expressed as mean ± S.E.M. n=6. [a]P<0.05 vs Sham; [b]P<0.05 vs MI. MI, myocardial infarction; PAG, propargylglycine; NaHS, sodium hydrosulfide.